

The biocompatibility of the precipitation-  
enhancing anodic oxidation on titanium  
implant material

Sunhong Hwang

The Graduate School

Yonsei University

Department of Dental Science

The biocompatibility of the precipitation-  
enhancing anodic oxidation on titanium  
implant material

Thesis supervisor; Professor Moon-Kyu Chung

A Dissertation

submitted to the Department of Dental Science and the  
Graduate School of Yonsei University in partial fulfillment of  
the requirements for the degree of Doctor of Philosophy

Sunhong Hwang

December 2005

This certifies that the dissertation of  
Sunhong Hwang is approved

Thesis supervisor: Moon-Kyu Chung \_\_\_\_\_

Thesis committee:

Ho Yong Lee \_\_\_\_\_

Kyoung Nam Kim \_\_\_\_\_

Yi Hyung Woo \_\_\_\_\_

Dong Hoo Han \_\_\_\_\_

The Graduate School

Yonsei University

December 2005

## 감사의 글

이 논문이 완성이 완성되기까지 도와주신 선생님들께 감사드립니다.  
이지환, 주옥현, 백민규선생님, 그리고 오근택 박사님.

부족한 부분을 채워주시고 조언해주신 지도교수님께 감사드립니다.  
이호용, 김경남, 정문규, 한동후, 우이형교수님.

부족한 저를 사랑으로 감싸주시고 격려해주신 부모님, 아내 정하에게  
감사드립니다.

작은 결실을 맺는 데는 참으로 많은 노력들이 있어야 하고, 그  
노력들은 혼자의 힘으로는 결코 이루어질 수 없다는 것을 깨닫게  
됩니다. 더불어 살아가는 지혜인 보편적인 가치가 자연과학의 한 쪽  
귀퉁이를 차지하고 있는 치과 보철학 분야에도 적용되고 있다는 것을  
생각하게 됩니다.

항상 저와 우리 가정을 지켜주시고 어긋날 때마다 바로 잡아주시는  
하나님께 감사드립니다.

## TABLE OF CONTENTS

LIST OF FIGURES .....	ii
LIST OF TABLES .....	iii
ABSTRACT (ENGLISH) .....	1
I. INTRODUCTION .....	3
II. MATERIALS AND METHODS .....	7
A. Sample preparation .....	7
B. Phase analysis .....	8
C. SEM(Scanning Electron Microscopy) .....	8
D. Cell proliferation .....	8
E. Bioactivity test .....	9
F. MTT test .....	9
<b>III. RESULTS .....</b>	<b>12</b>
A. Phase analysis.....	12
B. SEM.....	15
C. Cell proliferation.....	18
D. Bioactivity test.....	20
E. MTT test.....	21
<b>IV. DISCUSSION .....</b>	<b>23</b>
<b>V. CONCLUSION .....</b>	<b>30</b>
<b>VI. REFERENCES .....</b>	<b>31</b>
<b>ABSTRACT (KOREAN) .....</b>	<b>35</b>

## LIST OF FIGURES

Figure 1. Schematic diagram of the equipment for anodic oxidation...	11
Figure 2. XRD analysis of commercially pure titanium.....	13
Figure 3. XRD analysis of Anodic oxidation.....	14
Figure 4. XRD analysis of precipitation-enhancing anodic oxidation..	14
Figure 5, 6. SEM of anodic oxidation.....	16
Figure 7. SEM of precipitation-enhancing anodic oxidation.....	17
Figure 8. Mean of cell proliferation at day 2, 4, 6, and 8 for groups.....	19
Figure 9. SEM micrographs of specimens at day 2, 8, 16, and 32 for groups.....	20
Figure 10. Mean of cell viability (%) at 24h and 48h for groups.....	22

## LIST OF TABLES

Table 1. Surface treatment methods for groups.....	8
Table 2. Composition of SBF (simulated body fluid, pH; 7.4).....	10
Table 3. EDS (energy dispersion spectroscopy) analysis of group 2 and group 3.....	13

## ABSTRACT

### **The biocompatibility of the precipitation-enhancing anodic oxidation on titanium implant material**

The studies regarding the surface of titanium implant have focused on reducing the healing period of osseointegration from the early machined surface to the modified surface of numerous methods. Titanium as a bioinert material is material of choice due to bioinertness of titanium oxide. Moderately roughened surface of titanium is mainly anchored by biomechanical bonding. In order to achieve biochemical bonding, coating technique has been developed. However, hydroxyl apatite coating as a biochemical bonding has potential drawbacks like inconsistency of the crystallinity and delamination from the titanium surface.

Chemical modification of titanium surface is studied *in vitro* such as alkali heat treatment, and anodization. The aim of the present study was to analyze the biocompatibility of a novel anodic oxidation, which is called precipitation-enhancing anodic oxidation, compared with anodized and machined surface of titanium.

Specimens (10mm×10mm×1m, 5mm×5mm×1mm) are fabricated with commercially pure titanium and different surface treatments are done such as machined, anodic oxidation, and precipitation-enhancing anodic oxidation. Phase analysis, SEM, cell proliferation, bioactivity, and MTT test are examined to compare the biocompatibility of the specimens.

The results of the studied showed as follow

1. Phase analysis showed that anatase form of  $\text{TiO}_2$  was found in Group 2 (anodic oxidation) and Group 3 (precipitation-enhancing anodic oxidation), not in Group 1 (machined surface)
2. SEM photographs of Group 2 and Group 3 revealed that the size of the orifices was varied from  $0.2\mu\text{m}$  to  $3\mu\text{m}$ , predominantly in the range  $1-2\mu\text{m}$ . The pore structures were arranged irregularly without any



direction and the periphery of the pores were erupted slightly. The thickness of TiO<sub>2</sub> were expected to be around 7-10μm.

3. Cell proliferation, Bioactivity test, and MTT tests in this study confirm that precipitation-enhancing anodic oxidation has potential affinity and non-toxic to cell attachment and growth.

This preliminary work tried to observe the biocompatibility in novel anodic oxidation compared with anodic oxidation and machined titanium. After this preliminary study was done, more questions like what is the composition of precipitant, how well dose the precipitant remain in bone after the insertion of the implants, and what is the role of precipitant to enhance the osseointegration in living bone, need to be answered in the future study.

---

KEY WORDS: Anodic oxidation, Precipitation-enhancing anodic oxidation, titanium oxide, implant surface

# **The biocompatibility of the precipitation-enhancing anodic oxidation on titanium implant material**

*Department of Dental Science,  
Graduate School, Yonsei University  
(Directed by Prof. Moon-Kyu Chung, DDS., PhD)*

**Sunhong Hwang**

## **I. INTRODUCTION**

The studies regarding the surface of titanium implant have focused on reducing the healing period of osseointegration from the early machined surface to the modified surface of numerous methods.<sup>1</sup> The definition of the osseointegration has also been changed along with the development of the surface science in implant dentistry. Bränemark<sup>2</sup> defined that the osseointegration could be a direct structural and frictional connection between ordered, living bone and the surface of a load-carrying implant. Albrektsson et al<sup>3</sup> in 1987 stated that osseointegration might be a direct contact between a loaded implant surface and bone at the light microscopic level. The zone of amorphous material consisted of proteoglycans and glycosaminoglycans, has been found between the titanium oxide and bone matrix. Therefore, weak van der Waals bonding, direct chemical bonding, or a combination of the two are considered to influence the quality of osseointegration. The mechanism of the enhancing osseointegration by either modifying the design or changing surface characteristics of the implant has been developed and introduced to the market by dental implant companies without clinical documentation in advance.<sup>4</sup>

The clinically proven machined surface<sup>5</sup> was questioned in the area of the poor bone quality; therefore, the roughened surface either additive or

subtractive method had been paid attention to achieve stable and rapid osseointegration. Wennerberg et al<sup>6</sup> pointed out that the certain degree of roughness always exists in surface of implant even in machined surface. Implants with the roughness approximately 1.5 $\mu$ m in Sa value showed stronger bone response than smoother and rougher implants.

Titanium as a bioinert material is mainly anchored to bone by biomechanical bonding. However, bioactive materials such as hydroxyapatite, bioglass, and calcium phosphate ceramics have potential to elicit a specific biological response at the interface of the material which results in the formation of a bond between tissues and materials so called biochemical bonding. Hydroxyapatite surface coating on titanium is thought to be advantageous because both mechanical properties of titanium and biochemical bonding of hydroxyapatite to bone can be utilized in one place.<sup>7</sup> The concerns regarding hydroxyapatite plasma spray coating have been raised that the crystallinity of this coating are different among the implant system and delamination of coating layer may happen in clinical use.<sup>8,9</sup> Therefore, chemical modifications of titanium which may lead to bioactive material were attempted to study *in vitro*. Surface modifications have consisted of alkali (NaOH) and heat treatment, ion implantation with calcium, or anodizing with electrolytes containing phosphorus, sulphur, calcium, or magnesium.

Moderately roughened surfaces are currently put into market by most of the implant companies even though machined surfaces are clinically successful in long-term study.<sup>4,10</sup> In orthopedics, smooth surfaced implant placed in skeletal bones usually tend to be encapsulated by fibrous tissue and show only weak bonding to bone in animal experiments even under unloaded conditions.<sup>11</sup> Alkali and heat treatment had been developed alternative to hydroxyapatite spray coating method in orthopedics. The surface of the titanium forms bone-like apatite in simulated body fluid (SBF) after alkali and heat treatment. Apatite formation on the surface of alkali and heat treated titanium metals appears to occur *in vivo*, and leads to bonding to living bone.<sup>12</sup> Histological and histomorphological

evaluations in the animal study showed that direct bone contact with the implant surface was significantly higher in the alkali and heat treated implants than control implant without any treatments.<sup>13</sup> In another study by the same group, the bone-bonding shear strengths of the implant were evaluated using push-out test. The result of the study supported that the early and strong bonding to bone of alkali and heat treated titanium was expected than untreated one.<sup>14</sup>

One of modifying the surface characteristics of implant can be achieved by varying properties of the oxide films. Oxide layers normally form a protective film on titanium at the time of exposure to air and water content. The chemical composition of oxide films consist mainly of TiO<sub>2</sub>, a polymorphic substance presented in three crystalline phases; anatase, rutile, and brookite with different properties and structures.

Crystallinity and thickness of the oxide film are considered to play an important role in corrosion resistance<sup>15</sup>; therefore, the procedure of anodizing the titanium surface was introduced to improve the quality of oxide layer.<sup>16</sup> In the study of Sul et al, the anodic oxide formation was influenced by anodic forming voltage. The oxide thickness varied slightly according to the measuring areas and was thicker at thread-flanks than at the other measured areas of the screw implants. Moreover, an increase of the anodic forming voltage related to generate the pore or crater in irregular shape.<sup>17</sup> The surface roughness, oxide crystallinity, and surface composition of the anodic oxide were dependent on the voltage, current density and concentration of the electrolyte.<sup>18</sup> Changing the concentration of electrolyte can influence the crystallinity of oxide layer which is related to the calcium and phosphorus concentration.

Anodic oxidation is thought to be an effective way to enhance the osseointegration by modifying the thickness, structure, composition, and topography of titanium oxide. The long-term clinical use of anodizing surface is expected in the future. Precipitation-enhancing anodic oxidation has been developed to combine the advantage of the topographic features of anodic oxidation with chemical modification of the surface. The aim of the present study

was to analyze the biocompatibility of a novel anodic oxidation, which is called precipitation-enhancing anodic oxidation, compared with anodized and machined surface of titanium.

## II. MATERIALS AND METHODS

### A. Specimen preparation

Commercially pure titanium (grade III, ASTM F67 Allegheny, Pittsburgh, Pennsylvania, USA) was used to fabricate plates (10mm×10mm×1m, 5mm×5mm×1mm) as specimens. For the group 1 as the machined surface, specimens were polished with SiC paper of grit #600 and cleansed ultrasonically in acetone, ethanol, and distilled water in order for 10 min respectively.

For group 2 of the anodic spark deposition, the procedure of the surface treatment was as followed. Titanium plates were polished and cleansed ultrasonically after 1mm diameter of hole was made at the corner of the plate. Titanium wire was placed to hold the plate in the chamber. The titanium plate and platinum plate were connected at the anode and the cathode respectively. The electrolytes consisted of 0.04M beta-glycerol phosphate disodium salt n-hydrate (C<sub>3</sub>H<sub>7</sub>Na<sub>2</sub>O<sub>6</sub>P·nH<sub>2</sub>O, Fluka, Buch, Swiss) and 0.4M calcium acetate n-hydrate ((CH<sub>3</sub>COO)<sub>2</sub>Ca·nH<sub>2</sub>O, Junsei, Tokyo, Japan) in distilled water.

250V (constant voltage) for 3 min was chosen as anodization (anodic oxidation) condition by using power supply (Genesys 600-2.6, Densei-Lambda, Japan). During the anodization, the electrolytes were stirred with a magnetic bar in order to reduce the formation of the gas evaporation.

For the group 3 of precipitation-enhancing anodic oxidation, the composition of the electrolytes were modified from the one that used in group 2, but the anodization condition was same as group 2. For the control group, polystyrene coated glasses (10mm×10mm×1m, 5mm×5mm×1mm) were fabricated by cutting the slide glass and were cleansed ultrasonically.

Table 1. Surface treatment methods for groups

Group	Surface treatment
Group 1	Machined surface
Group 2	Anodic oxidation
Group 3	Precipitation-enhancing anodic oxidation
Group 4	Glass, control

## **B. Phase analysis**

X-ray diffraction analysis was conducted over a scan range of 10-80° at a scan rate of 4 °/min, using the K ray of a Cu target to identify phases of specimens (XRD, X-ray Diffraction, D-Max Rint 240 model, Rigaku Co., Japan). The JCPDS (Joint Committee on Powder Diffraction Standards) cards were used to index the X-ray diffraction peaks.

## **C. SEM(Scanning Electron Microscopy)**

Scanning electron microscopy (SEM, S-2700 model, Hitachi, Japan) was used to evaluate the surface morphology of the each group of specimens.

## **D. Cell proliferation**

6 Specimens per group were placed to 6 well plate for the evaluation of the cell proliferation. Cells (ST2) were cultured in  $\alpha$ -MEM (Modified Eagles's Essential Medium, Gibco, USA) containing 10% FBS (Fetal Bovine Serum) in a 37°C, 5% CO<sub>2</sub> incubator. 100  $\mu$ l of 1 $\times$ 10<sup>3</sup> cell/ml were seeded onto specimens in 6 well plate. The cells were cultured in CO<sub>2</sub> incubator for 2, 4, 6, and 8 days. The medium was replaced every 2 days. Cells were detached from the specimens by adding 1 ml of trypsin and supernatants were removed by the centrifuge. After mingling 1 ml of the medium, the number of cells in each

20  $\mu$ l was counted 10 times by the Haemocytometer and an average value of the counted number had calculated for comparison among groups.

#### **E. Bioactivity test**

The 4 specimens for each group were selected and placed in 2 specimens per vial for 2 vials per group. The vial was filled with 20 ml of a SBF, and kept in the water bath at 37°C. SBF was replaced every 2 days. Specimens were removed from vial at 2, 4, 6, 8, 16, and 32<sup>nd</sup> day, respectively. The surface morphology of specimens after bioactivity test was investigated by scanning electron microscopy (SEM, S-2700 model, Hitachi, Japan).

#### **F. MTT test**

MTT[3-(4,5-dimethylthiazol-2-yl)-2,5-diphenyl tetrazolium bromide] assay was performed to quantify cytotoxicity of specimen. MG-63 cells and DMEM were also used in MTT method. Specimens were ultrasonically degraded in 95% ethyl alcohol for 1 minute. The extracted liquid of specimens was made by autoclaving with DI (deionized) water (121°C, 1 hour). Cells were plated in 96-well at a density of approximately 10,000 cells/well, in medium for 24 hours in a 37°C, 5% CO<sub>2</sub> incubator. After incubation, extracted liquid was put in the well (0.18 ml/ well) and incubated in a 37°C, 5% CO<sub>2</sub> incubator. In control, only DI water was put in (0.18 ml/ well). After 5-hour incubation, 0.05 ml of MTT solution at concentration of 1 mg/ml in phosphate-buffered saline (PBS, Gibco, USA) was added to each well and allowed incubation for further 4 h. Since living cells metabolize the MTT in their mitochondria and form blue formazan crystals, 0.05 ml of DMSO (dimethylsulfoxide) was added to each well to dissolve the formed crystal. The wells were read at 570 nm on an ELISA plate reader and the percentage of cell viability was calculated. Cell viability of each groups were compared with control group. Statistical analysis was performed by two-way



analysis of variance (ANOVA) with Duncan's multiple range test to a significance level of  $P < 0.05$ .

Cell Viability = (spectrophotometric absorbance of group 1, 2 and 3 / spectrophotometric absorbance of group 4)  $\times$  100

Table 2. Composition of SBF (pH; 7.4)

sequence	medium	1ℓ
1	NaCl	7.996
2	NaHCO <sub>3</sub>	0.35
3	KCl	0.224
4	K <sub>2</sub> HPO <sub>4</sub> ·3H <sub>2</sub> O	0.174
5	MgCl <sub>2</sub> ·6H <sub>2</sub> O	0.305
6	1M-HCl	40 ml
7	CaCl <sub>2</sub>	0.278
8	Na <sub>2</sub> SO <sub>4</sub>	0.071
9	NH <sub>2</sub> C(CH <sub>2</sub> OH) 3	6.057

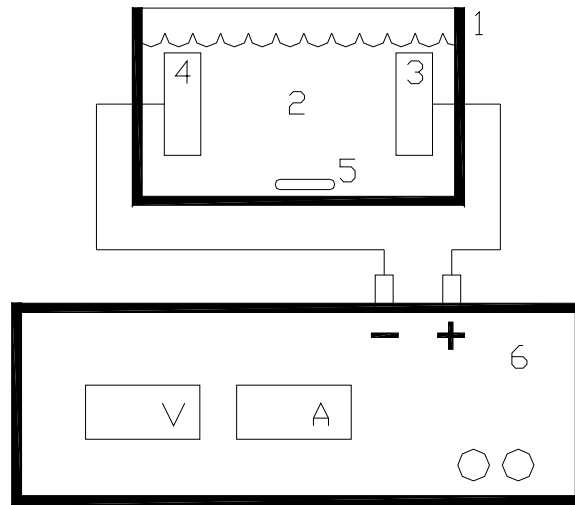


Figure 1. Schematic diagram of the equipment for anodic oxidation.

legend

1. electrolytic cell
2. electrolyte
3. anode (specimen)
4. cathode (usually Platinum (Pt) plate)
5. stirrer (magnetic bar)
6. DC power supply

### III. RESULTS

#### A. Phase analysis

X-ray diffraction analysis was conducted over a scan range of 10-80° at a scan rate of 4 °/min, using the K ray of a Cu target to identify phases of specimens (XRD, X-ray Diffraction, D-Max Rint 240 model, Rigaku Co., Japan). The JCPDS (Joint Committee on Powder Diffraction Standards) cards were used to index the X-ray diffraction peaks. The crystal structure of specimens was investigated by using X-ray diffraction analysis.

In group 2 of anodic oxidation, anatase structure of TiO<sub>2</sub> was found at the diffraction angle, 2 $\theta$  of 25.3 at the first peak but not in group 1 (Fig. 2). Titanium as a substrate was shown at the diffraction angle of 35, 40, and 54 (Fig. 3). In group 3 of precipitation-enhancing anodic oxidation, anatase structure of TiO<sub>2</sub> was also found at the diffraction angle of 25.3 (Fig. 4). The peaks showing Titanium substrate was found at the angle of 35, 40, and 54 respectively. This results indicated that the crystal structure of the group 2 and group 3 was similar and not influenced by the precipitant on the surface of group 3.

EDS (Energy dispersion spectroscopy) was used in order to understand the composition of the precipitant of the group 3. The surface areas of X-ray beam for EDS were greater than the size of the precipitant of Group 3, therefore it is impossible to examine the composition of the precipitant. However, the comparison between the group 2 and group 3 with EDS may implicate that the composition of the surface consisted of calcium, phosphate, and other elements. There was no distinct difference of composition of elements found between Group 2 and Group 3 in Table 3.

Table 3. EDS analysis of group 2 and group 3

specimen	Group 2	Group 3
precipitation elements	P:Ca	P:Ca
atomic ratio	1:2.22	1:1.84

Ca : O : P = 20.90 : 68.58 : 10.52

EDS on the Group 3.

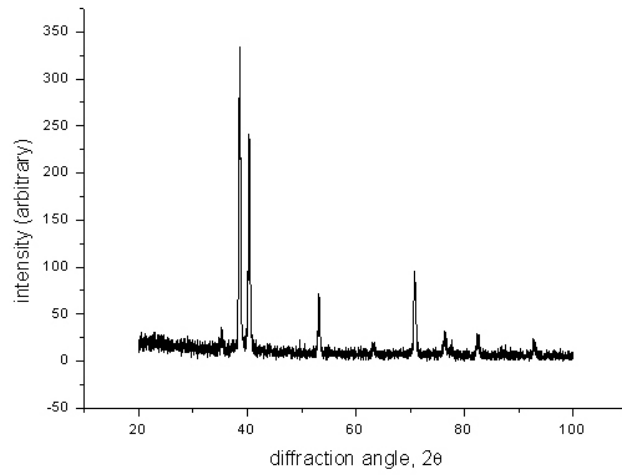
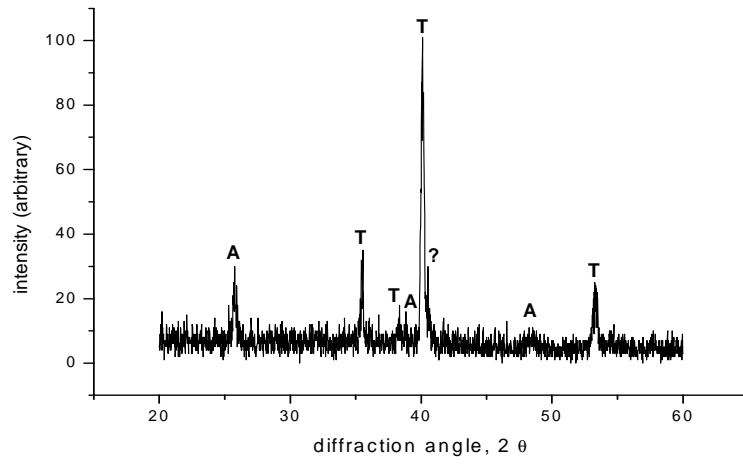
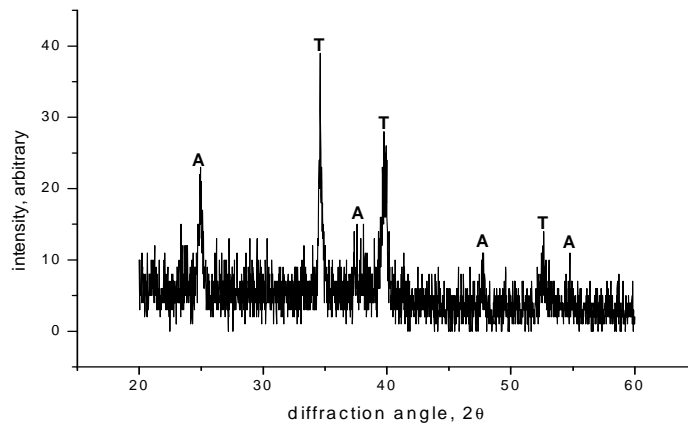


Figure 2. XRD pattern of commercially pure titanium(machined surface).



T: titanium, A: anatase (beta titanium dioxide, tetragonal) (TiO<sub>2</sub>)

Figure 3. XRD pattern of anodic oxidation.



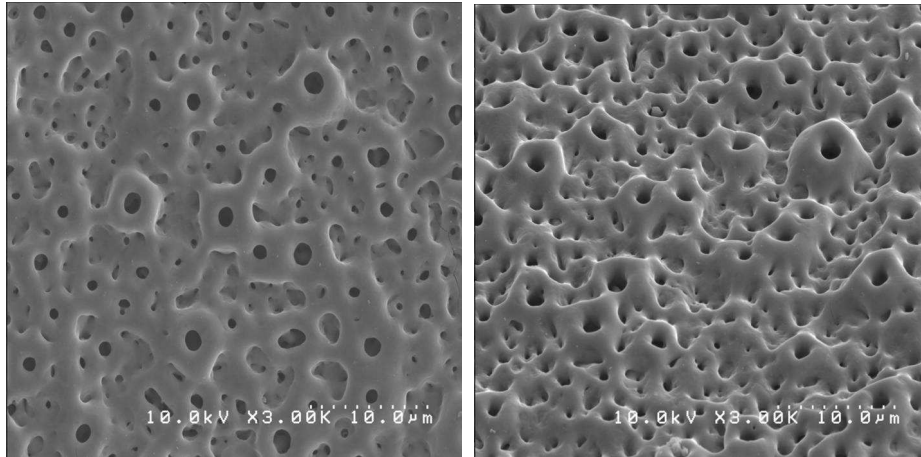
T: titanium, A: anatase (beta titanium dioxide, tetragonal) (TiO<sub>2</sub>)

Figure 4. XRD pattern of precipitation-enhancing anodic oxidation.

## **B. SEM (Scanning Electron Microscopy)**

Figure 5 and figure 6 showed SEM photographs of the surface of anodic oxidation at the magnification of  $\times 3,000$  and  $\times 30,000$  respectively. The surface showed a rough surface topography without sharp features and the surface contained numerous open pores or crater structures, generally round shape, with different sizes around 2-3 $\mu\text{m}$  diameter. The size of the orifices was varied from 0.2 $\mu\text{m}$  to 3 $\mu\text{m}$ , predominantly in the range 1-2 $\mu\text{m}$ . The pore structures were arranged irregularly without any direction and the periphery of the pores were erupted slightly. The thickness of  $\text{TiO}_2$  were expected to be around 7-10 $\mu\text{m}$ .

Figure 7 showed SEM photographs of the surface treated by precipitation-enhancing anodic oxidation at the magnification of  $\times 2,000$  and respectively. The topography of the specimens in group 3 was similar to that in group 2 in terms of the number and size of pores. However, the whitish granules were shown to be attached on specimens in group 3. At the magnification of  $\times 20,000$ , the granules also found to be attached inside of the craters or pores. The size of the granules were varied in the range 0.15 $\mu\text{m}$  to 0.45 $\mu\text{m}$ .



left:  $\times 3000$

right:  $\times 3000$  with oblique angulation

Figure 5. Anodic oxidation of specimen: cp-Ti grade III (ASTM F67)

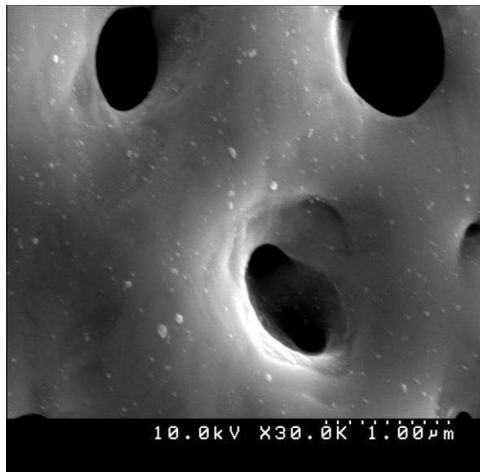
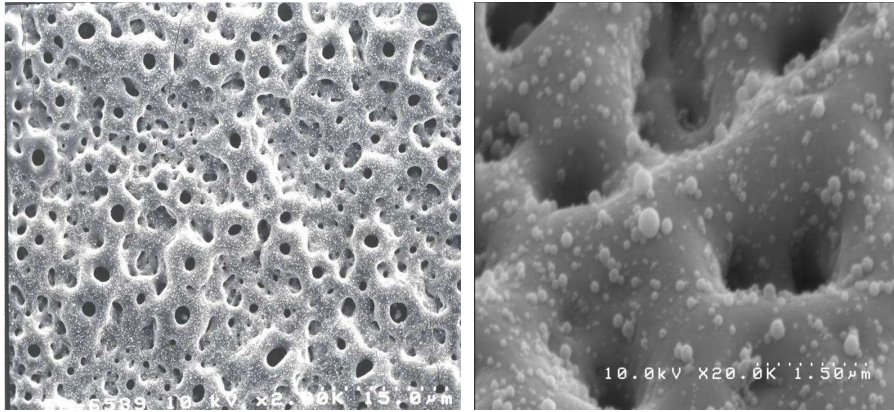


Figure 6. Anodic oxidation with the different magnification ( $\times 30000$ ).



left:  $\times 2,000$ ,

right:  $\times 20,000$

Figure 7. Precipitation-enhancing anodic oxidation of specimen: cp-Ti grade III (ASTM F67)



### **C. Cell Proliferation**

A two-way ANOVA was used to compute whether significant differences exist between cell proliferation of the groups to the day 2, 4, 6, 8 and Duncan's multiple range test was used to test when significant differences of cell proliferation happens at the observation period. The differences between 4 groups of cell proliferation were statistically significant and the significant differences were existed at the observation period. ( $P < 0.05$ )

Duncan's multiple range test revealed that the cell proliferation was significantly increased between day 4 and day 6 for all groups. In group 2 and group 4, the significant cell growth was also found between day 6 and day 8.

Results of Duncan's multiple range test for groups showed that there were significant differences between group 2 and group 3 at day 2 and day 4. The cell proliferation of group 3 was greater than that of group 2 at day 2 and day 4. At day 6, significant differences existed between group 2 and group 3, the number of cell counted in group 3 was greater than that of group 2. At day 8, there were no significant differences shown among groups. The least number of cell proliferation was found in group 2 during the observation period.

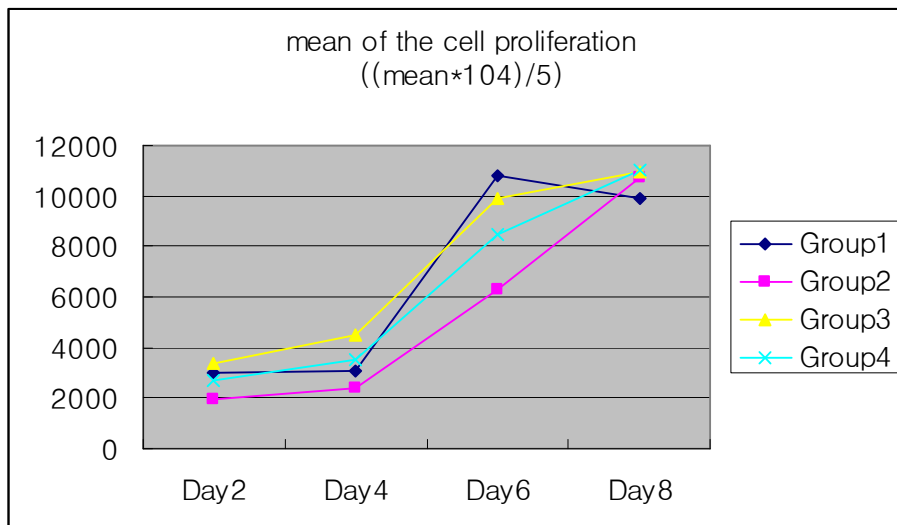


Figure 8. Mean of the cell proliferation at day 2, 4, 6, and 8 for groups.

#### D. Bioactivity test

Figure 9 showed SEM micrographs of the specimens of each group at the day of 2, 8, 16, and 32. After 2 days in SBF precipitants layer attached were observed only in Group 3. At day 8, 16 precipitants could be found on all of the groups as cluster shapes. At day 32, powder-shaped structures transformed to rod-shaped structures in Group 2 and 3, but in group 1 and 4 no changes were observed.

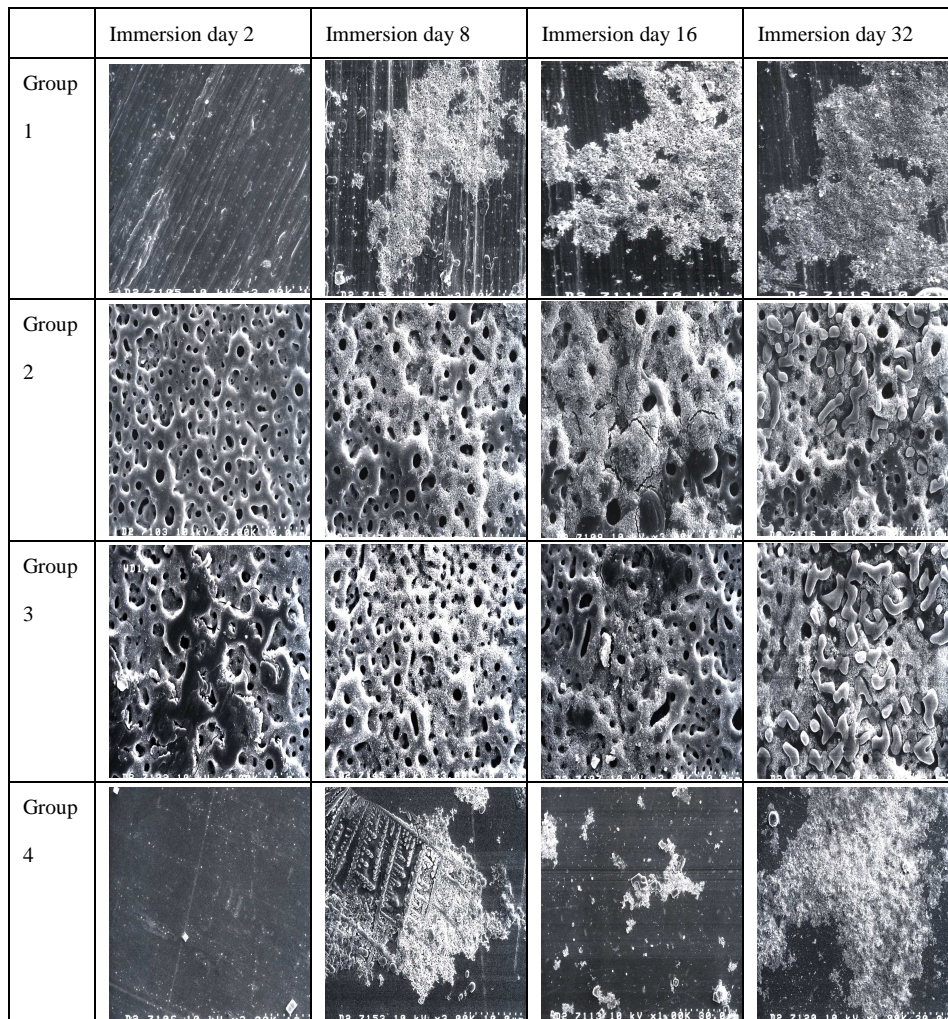


Figure 9. SEM micrographs of specimens at day 2, 8, 16, and 32 for groups.

## **E. MTT test**

The values of spectrophotometric absorbance in each group can be considered equivalent to the number of cells survived in the observation period. A two-way ANOVA with Duncan's multiple range test was performed to evaluate if the statistical significances can be found among groups and observation period. There was a significant differences noticed between groups and time at  $P < 0.05$ . However, Duncan's multiple range test revealed that there were not significant differences among groups at 24 h, but significant differences at 48 h. The value of optical density for group 2 was significant statistically higher than that for control group (group 4) at 48 h. There was no significant difference between group 1 and group 2 and group 3.

Considering the time factor, all of tested group and control group showed that the value of the optical density at 24 h was greater than one at 48 h. Duncan's multiple range test showed that the statistical significances were found all of groups tested between at 24h and at 48h. It may be concluded that ion release expected from all tested materials such as machined, anodization, and precipitation-enhancing anodic oxidation were too tiny amounts to jeopardize the cell survival.

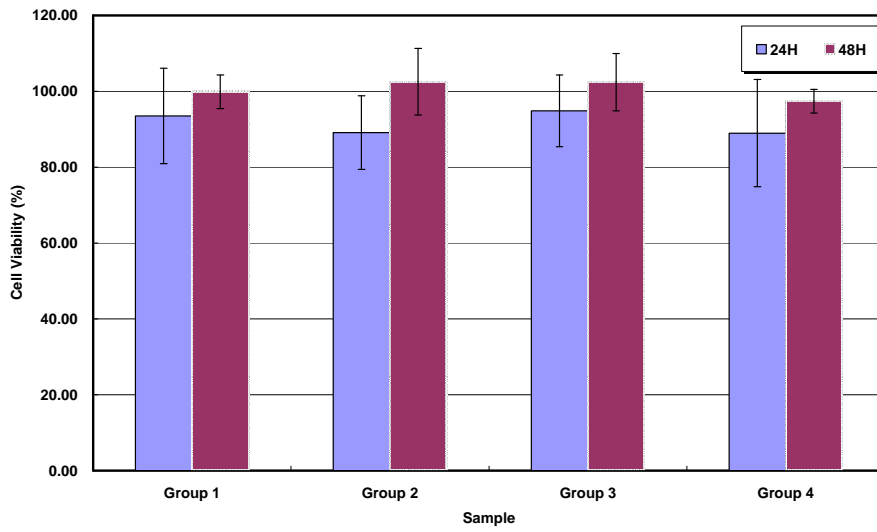


Figure 10. Mean of cell viability (%) at 24h and 48h for groups.

#### IV. DISCUSSION

The concept of osseointegration has been evolved through the efforts of the numerous researchers to find the way to reduce the healing time and secure the long-term success of the restoration supported by anchored implants. During the late 1960s, it was believed that successful healing of implant with bone occurred in case of the implant was encapsulated with fibrous tissue. The fibrous periimplant membrane with its shock-absorbing feature was preferable to implant fused to bone. But this fibro-integration ended up with high clinical failure rate so it is no longer considered adequate interface for implants.<sup>19</sup>

Bränemark defined that osseointegration as a “direct structural and frictional connection between ordered, living bone and the surface of a load-carrying implant.” Albrektsson et al. in 1987 stated that osseointegration is a direct contact between a loaded implant surface and bone at the light microscopic level. Performing a clinical mobility test and radiographic evaluation has been proposed to demonstrate osseointegration clinically. Mobile implant is definitely not osseointegrated, unfortunately the presence of clinical stability cannot be taken as conclusive evidence of osseointegration. Periotest and Resonance frequency analysis can be utilized to evaluate the status of implant placed in bone, however there is limitation of those method in daily practice. Radiolucent zones around the implant are a clear indication of its being anchored in fibrous tissue, whereas the lack of such zones is not evidence for osseointegration. The reason for this was that the optimal resolution capacity of radiography is in the range of 0.1 mm whereas the size of a soft tissue is in the range of 0.01 mm, therefore a narrow zone of fibrous tissue may be undetectable by radiography.<sup>3</sup> Some studies mentioned that the implants are usually supported by a composite of calcified bone, unmineralized osteoid matrix, and connective tissue. The true nature of the interface between implants and bone is yet to be determined. Nevertheless, ultrastructural investigations between implants and bone in areas of osseous integration reveal a zone of amorphous material at the interface of implant and

bone. This material has been reported to consist of proteoglycans and glycosaminoglycans as indicated by histochemical staining techniques. The exact chemical nature of interface that forms between this amorphous layer and the metallic implant surface is yet to be determined. It has been theorized, however, that weak van der Waals bonding, direct chemical bonding, or a combination of the two may be present. Moreover, it is still controversial whether commercially pure titanium forms a direct chemical bond to bone.<sup>20</sup>

Machined titanium surface demonstrated the long-term success rate of restoring fully edentulous patient at early studies where the bone quality and quantity was appropriate such as anterior mandible. The clinical results of machined surfaced implants could be compromised for areas with less dense bone like the posterior maxilla.<sup>21</sup>

In an attempt to improve the quantity and quality of the bone-implant interface, numerous implant surface modifications have been used. The method of surface modification can simply be categorized by either subtractive method or additive method. Subtractive methods consisted of acid etching, sandblasting, TiO blasting, and SLA(sandblasting and acid etching). The specific features of each methods above were different, but in general the matrix of the titanium surface was removed to form the designated characteristics of the implant surfaces. On the other hand, Additive methods were TPS and HA coating as well as sintering of spherical titanium alloy.<sup>22</sup> In these methods, particulate titanium alloys or hydroxyapatite would be attached on the surfaces of implants under high temperature and pressure. The characteristics of the surface could be dominated with the biochemical properties of the coatings, not strongly related with those of titanium itself.

Hydroxyapatite coatings on titanium were paid attention due to the advantage of the mechanical properties of titanium and biochemical bonding potential of hydroxyapatite in one place.<sup>7</sup> The properties of hydroxyapatite coatings on titanium are not same among the implant systems. HA-coated implant systems available in market varied with regard to the biochemical composition of

their HA coatings. HA coatings comprise varying percentage of crystalline hydroxyapatite, tricalcium phosphate(TCP), and amorphous calcium phosphate. Kim et al. reported that the crystalline nature of HA coatings in 4 different brands (Calcitek, Bio-vent, SteriOss, and Lifecore Biomedical) ranged between 30% and 66%, with varying percentages of crystalline HA, TCP, and amorphous calcium phosphate. It is believed that more crystalline HA implant coating contains, better resistant to dissolution of coating will be. Conversely, increased concentrations of amorphous calcium phosphate and TCP are thought to predispose the hydroxyapatite coating to dissolution.<sup>23</sup> Several studies showed that HA coated implants compared with non-coated titanium implants had demonstrated superior early bone contact and reached shear bonding strength faster.<sup>24</sup> However, whether these advantages of hydroxyapatite coatings on titanium can persist clinically is controversial.<sup>25</sup>

The modified topography either subtractive or additive method of titanium were compared, in animal and human clinical studies, with control of machined surface of implant regarding removal torque values, bone to implant contacts, Periotest, and RFA. Summarizing these studies, it can be concluded that titanium implants with modification achieve a significantly faster and better anchorage in bone when compared with titanium implants with smooth or fine structured surface.<sup>26,27,28,29</sup>

Smooth surfaced implant placed in skeletal bones usually tend to fail due to fibrous encapsulation, therefore the chemical modification of the implant surface were needed to achieve the clinical success of implant. Alkali and heat treatment has been studied alternative to hydroxyapatite spray coating method.<sup>13,14</sup> The mechanism of hydroxyapatite formation on the NaOH and heat treated titanium soaked in SBF (simulated body fluid) was explained as follow. NaOH-Ti surface possessed the capability to induce a Ca-P coating on the titanium surface. Octacalcium phosphate (OCP) crystals were first grown on a NaOH-Ti surface, followed by hydroxyapatite (HA) with a preferential orientation on OCP. It is found that two factors controlled the growth of Ca-P



crystals on NaOH-Ti from SBF. First, the surface morphology of NaOH-Ti characterized with crevices seems to be beneficial for inducing a Ca-P coating from SBF; second, the basic hydroxyl, Ti-OH, radical has increased in NaOH-Ti with the increase of treating time and concentration, which facilitate the nucleation of Ca-P crystals.<sup>30</sup> However, Clinical usage of the implant surface treated with alkali and heat treatment was not published in the literature.

One aim of current implant researches is to design a surface with topographical and chemical properties that accelerate the healing period of osseointegration. Anodic oxidation is one technique for surface modification of titanium and results in an increased thickness of the native oxide layer and changes surface topography.<sup>31,32</sup> That is why anodic oxidation can be considered as additive method of surface modification.

The characteristic properties of the anodic oxidation surface of dental implant in market are summarized as follows: (1) the surface consisted of an essentially pure partly crystalline TiO<sub>2</sub>. The oxide thickness increased continuously from 1-2 μm at the upper part to 7-10 μm at the apical aspect of the implant; (2) The surface roughness and area increased continuously from the flange to the apical part of the implant, where surface roughness was 1.2 μm and area increase compared with an ideally flat surface was 95 % ; (3) The surface showed a rough surface topography without sharp features; and (4) The surface (apical portion) contained numerous open pores, with orifices predominantly in the range 1-2 μm.<sup>31,32</sup> Ivanoff et al. showed that histological biopsies in human jawbone demonstrated a significantly higher bone response for anodic oxidized titanium implants than for implants with a turned surface. The reason for this result may depend on one or multiple differences of the surfaces between test and control implants: (1) the thicker oxide layer itself, (2) increased surface roughness, (3) different surface morphology in terms of porosity, or (4) change in crystal structure.<sup>33</sup> Schüpbach et al. reported that the clinically retrieved oxidized implants showed evidence of bone growth into the pores, including pores with small diameters (< 2 μm), of the surface oxide layer with SEM. The authors

mentioned that those findings indicate the establishment of a strong interlock between the bone and the oxidized titanium implant, which is suggested to be beneficial performance.<sup>34</sup>

Precipitation-enhancing anodic oxidation has been developed to combine the advantage of the topographic features of anodic oxidation with chemical modification of the surface. This research can be regarded as preliminary experiments to see the biocompatibility of the novel anodic oxidation compared with anodized and machined surface of titanium.

In phase analysis, the oxide layer of TiO<sub>2</sub> for group 2 (anodic oxidation) and group 3 (precipitation-enhancing anodic oxidation) revealed the anatase structure of TiO<sub>2</sub> was found at the diffraction angle, 2 $\Theta$  of 25.3 at the first peak. It is well known that exposed surfaces of titanium spontaneously are covered by a 3-6nm layer of titanium oxide, mostly as amorphous titania.<sup>35</sup> TiO<sub>2</sub> is known for its polymorphism mostly anatase, rutile, and brookite. Brookite is less-common phases. Anatase has been identified as the metastable form of TiO<sub>2</sub> and can be converted rutile, stable form and bioinert, at 700°C.<sup>36</sup> Metastable form of TiO<sub>2</sub> with high surface energy is thought to elicit more active cellular responses than stable form of TiO<sub>2</sub>. (Figure 3, 4)

SEM photographs (Figure 5,6) of the surface of anodic oxidation showed a rough surface topography without sharp features and the surface contained numerous open pores or crater structures, generally round shape, with different sizes around 2-3 $\mu$ m diameter. The size of the orifices was varied from 0.2 $\mu$ m to 3 $\mu$ m, predominantly in the range 1-2 $\mu$ m. The thickness of TiO<sub>2</sub> was expected to be around 7-10 $\mu$ m. These findings were in accordance with the study by Hall and Lausmaa.<sup>31</sup>

SEM photographs (Figure 7) of the surface treated by precipitation-enhancing anodic oxidation showed that the topography of the specimens in group 3 was similar to that in group 2 in terms of the number and size of pores. However, the whitish granules were shown to be attached on specimens in group

3. The composition of the precipitant was speculated to be calcium and phosphate by EDS analysis. (Table 3)

Zhu et al.<sup>37</sup> reported that anodic oxide film containing Ca and P of titanium can be obtained with the electrolyte, 0.02 M calcium glycerophosphate and 0.15 calcium acetate, current density 70A/m<sup>2</sup>, and final voltage 350V. However, the surface of anodization of Zhu's study did not contain the whitish granule on the titanium showed on Figure 7 in this study.

Calcium ion-deposited implants using macro arc oxidation tested in the animal study, the results showed fast and strong osseointegration. Plausible explanations of the role of calcium in bone physiology were summarized by Sul et al. (1) Ca may facilitate the attachment of cells (osteoblast) via activation of integrin structures and thereby bind to RGD domain (Arginine-Glycine-Aspartic-acid) of adhesive proteins (fibronectin, vitronectin, osteopontin). (2) surface Ca chemistry of Ca implants incorporated into TiO<sub>2</sub> may form an electrostatic bond with polyanionic Ca<sup>+</sup> binding proteins such as proteoglycan, osteocalcin, osteopontin and osteonectin in bone matrix. (3) Ca cations in the Ca implant may provide the binding sites involved in any stages of the biologic mineralization pathway for a variety of Ca phosphate mineral forms.<sup>38</sup> The important role of Ca in the process of osseointegration explained above may support the concept of developing the precipitation-enhancing anodic oxidation which possessed precipitants of Ca and phosphate attached on the surface of anodic oxidation.

Cell proliferation, Bioactivity test, and MTT tests in this study confirmed that precipitation-enhancing anodic oxidation had a potential affinity and non-toxic to cell attachment and growth. However, there were no significant differences between anodic oxidation and precipitation-enhancing anodic oxidation at the longer observation period such as 48h cell proliferation, 32 day in SBF, MTT test 48 h. Cell proliferation at the early observation periods such as day 2 and day 4 showed that there were significantly greater cell proliferation in group 3 than that in group 2. The cell proliferation of group 3 was greater than that of group 2 at day 2 and day 4. This result might be speculated that the role of

calcium in bone physiology facilitated the attachment and initial growth of cell in group 3 which contained lots of precipitants on the surface.<sup>38</sup> Bioactivity test also showed that apatite precipitation was induced with the group 3, not the other groups at the early observation of day 2. For a bioactive material, the ability of the surface to induce apatite precipitation as well as the rate of apatite formation is very important. The composition of the apatite precipitant was not evaluated in this study. Jonasova et al. showed that the titanium can form a bone-like apatite layer on its surface in SBF when it is treated in NaOH.<sup>39</sup> The morphology of precipitant in the study of Jonasova was similar to one in this study. Therefore, it could be concluded that the precipitation-enhancing anodic oxidation was more bioactive than other surface treatment in this experiment.

This preliminary works tried to analyse the biocompatibility in a novel anodic oxidation compared with anodic oxidation and machined titanium. The results of this experiment may open the possibility of developing the novel anodic oxidation of titanium which contains a lot of precipitants thought to be calcium and phosphates. However, after this preliminary study was done, more questions like what is the composition of precipitant, how well dose the precipitant remain in bone after the insertion of the implants, and what is the role of precipitants to enhance the osseointegration in living bone, remained to be answered in the future study.

## V. CONCLUSION

The purpose of this preliminary study is to evaluate the biocompatibility of the surface modification of titanium, which is called precipitation-enhancing anodic oxidation, with machined surface and anodic oxidation of titanium plate. Specimens (10mm×10mm×1m, 5mm×5mm×1mm) are fabricated with commercially pure titanium and different surface treatments are done such as machined, anodic oxidation, and precipitation-enhancing anodic oxidation. Phase analysis, SEM, cell proliferation, bioactivity test, and MTT test are examined to compare the biocompatibility of the specimens.

Within the limitation of this study, the following conclusion may be made;

1. Phase analysis showed that anatase form of TiO<sub>2</sub> was found in Group 2 (anodic oxidation) and Group 3 (precipitation-enhancing anodic oxidation), not in Group 1 (machined surface)
2. SEM photographs of Group 2 and Group 3 revealed that the size of the orifices was varied from 0.2μm to 3μm, predominantly in the range of 1-2μm. The pore structures were arranged irregularly without any direction and the periphery of the pores were erupted slightly. The thickness of TiO<sub>2</sub> were expected to be around 7-10μm.
3. Cell proliferation, bioactivity, and MTT tests in this study confirmed that precipitation-enhancing anodic oxidation had a potential affinity and non-toxic to cell attachment and growth.

This preliminary works tried to observe the biocompatibility in a novel anodic oxidation compared with anodic oxidation and machined titanium. After this preliminary study was done, more questions like what is the composition of precipitant, how well dose the precipitant remain in bone after the insertion of the implants, and what is the role of precipitant to enhance the osseointegration in living bone, remained to be answered in the future study.

## VI. REFERENCES

1. Adell R, Lekholm U, Rockler B, Bränemark PI. A 15-year study of osseointegrated implants in the treatment of the edentulous jaw. *Int J Oral Surg* 1981; 10: 387-416.
2. Bränemark PI. Osseointegration and its experimental background. *J Prosthet Dent* 1983;50:399-410.
3. Albrektsson T, Jacobsson M. Bone-metal interface in osseointegration. *J Prosthet Dent* 1987;57:597-607.
4. Albrektsson T, Wennerberg A. Oral implant surfaces: part 2-review focusing on clinical knowledge of different surfaces. *Int J Prosthodont* 2004;17:544-564.
5. Eckert SE, Parein A, Myshin HL, Padilla JL. Validation of dental implant systems through a review of literature supplied by system manufacturers. *J Prosthet Dent* 1997;77:271-279.
6. Wennerberg A. On surface roughness and implant incorporation(thesis). Göteborg, Sweden:Department of Biomaterials, University of Göteborg, 1996:1-196.
7. Geesink RG, de Groot K, Klein CP. Bonding of bone to apatite-coated implants. *J Bone Joint Surg(Br)* 1988;70:17-22.
8. Ogiso M, Yamashita Y, Matsumoto T. The process of physical weakening and dissolution of the HA-coated implant in bone and soft tissue. *J Dent Res* 1998;77:1426-1434.
9. Overgaard S, Soballe K, Lind M, Bunger C. Resorption of hydroxyapatite and fluorapatite coatings in man. An experimental study in trabecular bone. *J Bone Joint Surg(Br)* 1997;79:654-9.
10. Lekholm U et al. Survival of the Bränemark implant in partially edentulous jaws: a 10-year prospective multicenter study. *Int J Oral Maxillofac Implants* 1999;14:639-45.
11. Spivak JM, Ricci JL, Blumenthal NC, Alexander H. A new canine model to evaluate the biological response of intramedullary bone to implant materials and surfaces. *J Biomed Mater Res* 1990;24:1121-49.
12. Kokubo T, Miyaji F, Kim H-M, Nakamura T. Spontaneous apatite formation

- on chemically surface treated Ti. *J Am Ceram Soc* 1996;79:1127-9.
13. Nishiguchi S, Kato H, Neo M, Oka M, Kim HM, Kokubo T, Nakamura T. Alkali- and heat-treated porous titanium for orthopedic implants. *J Biomed Mater Res* 2001;54:198-208.
  14. Nishiguchi S, Kato H, Fujita H, Oka M, Kim HM, Kokubo T, Nakamura T. Titanium metals form direct bonding to bone after alkali and heat treatments. *Biomaterials* 2001;22:2525-2533.
  15. Solar RJ, Pollack SR, Korostoff E. In vitro corrosion testing of titanium surgical implant alloys: an approach to understanding titanium release from implants. *J Biomed Mater Res* 1979;13:217-50.
  16. Pankuch M, Bell R, Melendres CA. Composition and structure of the anodic films on titanium in aqueous solutions. *Electrochimica Acta* 1993;38:2777-2779.
  17. Sul YT, Johansson CB, Petronis S, Krozer A, Jeong Y, Wennerberg A, Albrektsson T. Characteristics of the surface oxides on turned and electrochemically oxidized pure titanium implants up to dielectric breakdown: the oxide thickness, micropore configurations, surface roughness, crystal structure and chemical composition. *Biomaterials* 2002;23:491-501.
  18. Zhu X, Ong JL, Kim S, Kim K. Surface characteristics and structure of anodic oxide films containing Ca and P on titanium implant material. *J Biomed Mater Res* 2002;60:333-338.
  19. Linkow LI. Endosseous oral implantology; a 7-year progress report. *Dent Clin N Am* 1970;14:185-200.
  20. Block MS, Kent JN: Endosseous implants for maxillofacial reconstruction. 1<sup>st</sup> ed. 1995, pp. 45-46, W.B. Saunders Company, Philadelphia, USA.
  21. Jaffin RA, Berman CL. The excessive loss of Brånemark fixtures in type IV bone: a 5-year analysis. *J Periodontol* 1991;62:2-4.
  22. Deporter DA, Todescan R, Watson PA, Pharoah M, Levy D, Nardini K. Use of the Endopore dental implant to restore single teeth in the maxilla: protocol and early results. *Int J Oral Maxillofac Implants* 1998;13:263-272.
  23. Kim Y, LeGeros J, LeGeros R. Characterization of commercial HA-coated dental implant [abstract 287]. *J Dent Res* 1994;73:137.
  24. Weinlaender M, Kenney EB, Lokovic V, Beumer J, Moy PK, Lewis S.

- Histomorphometry of bone apposition around three types of endosseous dental implants. *Int J Oral Maxillofac Implants* 1992;7:491-496.
25. Kent JN, Block MS, Finger IM, Guerra L, Larsen H, Misiak DJ. Biointegrated hydroxylapatite-coated dental implants: 5-year clinical observations. *J Am Dent Assoc* 1990;121:138-144.
  26. Klokkevold PR, Nishimura RD, Adachi M, Caputo A. Osseointegration enhanced by chemical etching of the titanium surface; a torque removal study in the rabbit. *Clin Oral Impl Res* 1997;8:442-447.
  27. Buser D, Nydegger T, Oxland T, Cochran DL, Schenk RK, Hirt HP, Snetivy D, Nolte LP. Interface shear strength of titanium implants with a sandblasted and acid-etched surface: a biomechanical study in the maxilla of miniature pigs. *J Biomed Mater Res* 1999;45:75-83.
  28. Wennerberg, Ektessabi, Albrektsson, Johansson, Andersson. A 1-year follow-up of implants of differing surface roughness placed in rabbit bone. *Int J Oral Maxillofac Implants* 1997;12:486-494.
  29. Xiropaidis AV, Qahash M, Lim WH, Shanaman RH, Rohrer MD, Wikesjö UME, Hall J. Bone-implant contact at calcium phosphate-coated and porous titanium oxide (TiUnite™)-modified oral implants. *Clin Oral Impl Res* 2005;16:532-539.
  30. Feng QL, Wang H, Cui FZ, Kim TN. Controlled crystal growth of calcium phosphate on titanium surface by NaOH-treatment. *J Crystal Growth* 1999;200:550-557.
  31. Hall J, Lausmaa J. Properties of a new porous oxide surface on titanium implants. *Appl Osseointegration Res* 2000;1:5-8.
  32. Larsson C. The interface between bone and implants with different surface oxide properties. *Appl Osseointegration Res* 2000;1:9-14.
  33. Ivanoff CJ, Widmark G, Johansson C, Wennerberg A. Histologic evaluation of bone response to oxidized and turned titanium micro-implants in human jawbone. *Int J Oral Maxillofac Implants* 2003;18:341-348.
  34. Schüpbach P, Glauser R, Rocci A, Martignoni M, Sennerby L, Lundgren AK, Gottlow J. The human bone-oxidized titanium implant interface: a light microscopic, scanning electron microscopic, back-scatter scanning electron microscopic, and energy-dispersive X-ray study of clinically retrieved dental implants. *Clin Implant Dent Related Research*. 2005;7(supplement1):S36-S43.



35. Sundgren J, Bodö P, Lundström I. Auger electron spectroscopic studies of the interface between human tissue and implants of titanium and stainless steel. *J Colloid Interface Sci* 1986;110:9-20.
36. Seo DS, Lee JK, Kim H. Synthesis of TiO<sub>2</sub> nanocrystalline powder by aging at low temperature. *J crystal growth* 2001;233:298-302.
37. Zhu X, Kim KH, Jeong Y. Anodic oxide films containing Ca and P of titanium biomaterial. *Biomaterials* 2001;22:2199-2206.
38. Sul YT, Johansson CB, Albrektsson T. Oxidized titanium screws coated with calcium ions and their performance in rabbit bone. *Int J Oral Maxillofac Implants* 2002;17:625-634.
39. Jonasova L Müller FA, Helebrant A, Strnad J, Greil P. Hydroxyapatite formation on alkali-treated titanium with different content of Na<sup>+</sup> in the surface layer. *Biomaterials* 2002;23:3095-3101.

국문요약

## 침전강화 양극 산화법으로 처리한 티타늄 금속의 생체 친화성 분석

임플란트 표면처리법에 대한 연구는 다양한 방법을 통해서 궁극적으로 골유착 과정을 빠르고 견고하게 이루려는 데 있다. 초기의 기계가공된 면에서 중등도의 거친 표면이 선호도를 갖게 되었다. 티타늄은 산화막의 생체 불활성의 성질 때문에 최선의 재료로 선택되었다. 중등도로 거친면을 갖는 티타늄 임플란트는 주로 기계적인 결합에 의해 즉 거친 표면과 골간의 결합에 의해 골유착을 이룬다. 생화학적인 결합력을 얻기 위해서 금속표면에 Hydroxyapatite를 입히는 방법등이 고안되었다. 그러나 이 방법의 문제점은 Hydroxyapatite의 결정구조가 일정치 않은 것과 생체내에서 표면이 떨어져 나오는 점이 생긴다. 이런 단점을 보완하기 위해서 티타늄표면의 화학적 변화를 주는 표면 처리법이 연구되었고, 알카리 열 처리법, 양극 산화법 등이 그 예이다.

이 번 연구의 목적은 양극 산화법에 화학적 변화를 발생한 침전강화 양극 산화법으로 처리한 티타늄 금속의 생체 친화성을 기계가공된 표면과 양극 산화법으로 처리된 표면과 비교하여 연구함이다.

시편은(10mm×10mm×1mm, 5mm×5mm×1mm) 상업적순수 티타늄으로 제작되고 표면처리는 기계 가공면, 양극 산화법, 침전강화 양극 산화법으로 처리하였다. 분석을 위한 방법으로. 상 분석, SEM, 세포 증식도, 생체 활성도, 세포 독성검사 등이 이용되었다.

연구 결과는 다음과 같다.

1. 상 분석 결과 Group 2 와 Group 3에 분석된 산화막의 결정구조는 Anatase로 나타났으나. Group 1의 경우는 Anatase구조가 발견되지 않았다.

2. Group 2 과 Group 3의 SEM 분석결과는 형성된 pore의 크기가 직경 0.2 $\mu\text{m}$  에서 3 $\mu\text{m}$  까지 다양하고 주로 1-2 $\mu\text{m}$ 의 크기가 관찰되었다. 관찰된 pore의 분포는 방향성을 갖지 않고 날카로운 구조는 보이지 않았으며, 분화구 모양의 형태를 보여준다. 산화막의 두께는 7-10 $\mu\text{m}$  정도로 관찰되었다.
3. 세포 증식도, 생체 활성도, 세포 독성검사의 결과는 침전강화 양극 산화법이 초기에 생체 반응에 우수한 결과를 보이거나 장기적 관찰결과에는 차이가 없고, 용출액을 이용한 세포 독성검사에도 독성이 없는 것으로 나타났다.

이번 실험의 결과를 토대로 침전강화 양극 산화법이 골유착에 유리한 조건을 갖는가에 대한 보다 심도 있는 연구가 필요하다고 사료되고, 특히 침전물이 표면에 어떻게 부착되는지 임플란트 식립 후에도 침전물이 남아있고, 골유착 과정에 어느 역할을 담당하는 지 등에 대한 연구가 요구된다.

---

KEY WORDS: 양극 산화법, 침전강화 양극 산화법, 임플란트 표면처리